

MINISTRY OF EDUCATION
AND TRAINING

VIETNAM ACADEMIC OF SCIENCE
AND TECHNOLOGY

GRADUATE UNIVERSITY OF SCIENCE AND TECHNOLOGY

Nguyen Thi Van Anh

**STUDY ON SYNTHESIS OF FERRATE (FeO_4^{2-}) SOLUTION
BY ELECTROCHEMICAL METHOD AND
APPLICATION FOR WASTEWATER TREATMENT**

SUMMARY OF DISSERTATION ON SCIENCES OF MATTER

Major: Theoretical and physical chemistry

Code: 9.44.01.19

Hanoi - 2025

The dissertation is completed at: Graduate University of Science and Technology, Vietnam Academy of Science and Technology

Supervisor 1: Dr. Mai Thi Thanh Thuy

Supervisor 2: Prof.Dr. Phan Thi Binh

Reviewer 1:

Reviewer 2:

Reviewer 3:

The dissertation is examined by Examination Board of Graduate University of Science and Technology, Vietnam Academy of Science and Technology at.....

The thesis can be found at:

- Library of Graduate University of Science and Technology
- National Library of Vietnam

LIST OF THE PUBLISHED PAPERS RELATED TO THE DISSERTATION

1. Thi Thanh Thuy Mai, **Thi Van Anh Nguyen**, Thi Binh Phan, Truong Giang Le, Ductile Iron: A Low-Cost Optimal Anode Material for Electrochemical Generation of Ferrate(VI), *Journal of The Electrochemical Society*, **2023**, 170, 8, 83510. (ISI, Q1).
2. **Thi Van Anh Nguyen**, Thi Thanh Thuy Mai, Thi Binh Phan, Huu Quang Tran, Minh Quy Bui, Ferrate(VI) green oxidant: electrochemical generation, self-decomposition, and application for reactive red 195 azo dye treatment, *J Chem Technol Biotechnol*, **2024**, 99, 2454–2463, (ISI, Q1).
3. Thi Thanh Thuy Mai, **Thi Van Anh Nguyen**, Thi Binh Phan, Effect of anode passivation on ferrate(VI) electro-generation using ductile iron anode and application for methylene blue treatment, *Journal of Applied Electrochemistry*, **2024**, 54, 1783–1794. (ISI, Q2).
4. **Nguyen Thi Van Anh**, Phan Thi Binh, Mai Thi Xuan, Mai Thi Thanh Thuy, The effect of NaOH concentration on ferrate electrosynthesis, *Vietnam J. Chem*, **2024**, 62, 4, 437-445. (Scopus, Q3).
5. **Nguyen Thi Van Anh**, Phan Thi Binh, Tran Huu Quang, Nguyen The Duyen, Phan Hoang Yen, Mai Thi Thanh Thuy, Efficient removal of methyl orange by ferrate(vi), *Vietnam journal of sciences and technology*. (VAST1, Scopus, accepted)
6. **Nguyễn Thị Vân Anh**, Mai Thị Thanh Thùy, Phan Thị Bình, Nghiên cứu tính chất điện hóa và quá trình tổng hợp ferrate (VI) trên điện cực anot gang xám trong môi trường kiềm đặc, *Tạp chí khoa học và công nghệ Việt Nam*, DOI: 10.31276/VJST.2025.2998.

INTRODUCTION

The rapid growth of the textile industry places a heavy burden on the environment due to the large volumes of wastewater discharged into natural water bodies. According to a report by the World Bank, textile industry effluents account for approximately 20% of global industrial wastewater. This wastewater contains hazardous organic dyes that severely disrupt aquatic ecosystems and pose serious health risks to humans. High concentrations of dyes in water sources reduce light penetration, impairing photosynthesis in aquatic plants and adversely affecting their growth and survival. Moreover, exposure to dye-contaminated water can lead to various health issues, including skin diseases, respiratory problems, and gastrointestinal disorders.

Azo dyes, which contain one or more stable azo groups ($-N=N-$), account for up to two-thirds of all synthetic dyes and are widely used in the textile, leather, and paper industries. The removal of azo dyes from wastewater has become an urgent challenge, attracting the attention of the scientific community and environmental protection organizations worldwide. Various methods have been applied to treat dye-contaminated wastewater, including Fenton and modified Fenton reactions, electrochemical processes, coagulation, biological treatments, adsorption, and photocatalysis. However, these methods often suffer from limitations such as the generation of secondary pollutants, long treatment times, or complicated material synthesis processes. Recently, ferrate(VI) oxidation has gained significant attention for the treatment of organic dyes due to its advantageous properties. Ferrate(VI) is a strong oxidizing agent with a redox potential as high as 2.2 V in acidic media, enabling it to efficiently degrade a wide range of toxic chemicals within a short time. Compared to other oxidants such as ozone, sodium hypochlorite (NaClO), and Fenton's reagent, ferrate has demonstrated superior treatment efficiency. Moreover, ferrate is regarded as a green oxidant because its reduction product, $\text{Fe}(\text{OH})_3$, is an environmentally friendly coagulant. Therefore, ferrate serves multiple roles in wastewater treatment, including acting as an oxidant, disinfectant, decolorizing agent, and coagulant.

There have been three primary techniques for synthesizing ferrate: electrochemical synthesis, thermal synthesis, and wet chemical synthesis. By comparing and evaluating the advantages and disadvantages of various ferrate synthesis methods, several limitations of the wet chemical method

and the thermal method are clear. The wet chemical method has low efficiency and produces many by-products, necessitating an additional purification step to remove excess products after synthesis. The thermal method has low reaction efficiency, is performed at high temperatures posing a risk of fire and explosion, and consumes a lot of energy. Meanwhile, the electrochemical method has recently emerged as a simple method that does not use chemicals and has no toxic by-products, a short synthesis time, and low cost. In addition, the electrochemical method can be used to synthesize ferrate in-situ for direct treatment of polluted wastewater sources, thereby addressing the instability of ferrate and difficulties in storage and transportation.

Therefore, the topic "*Study on the synthesis of ferrate solution (FeO_4^{2-}) by electrochemical method and its application for wastewater treatment*" is proposed.

Research objectives of the dissertation

- To determine the optimal conditions for ferrate synthesis using the electrochemical method.
- To determine the stability of ferrate.
- To apply the synthesized ferrate in the treatment of azo dyes.

Research content of the dissertation

- Study on the conditions affecting the process of ferrate synthesis by electrochemical method including: anode material, electrolyte, electrolysis time, current density, temperature.
- Study on the formation of a passive layer on the anode surface: Study the electrochemical properties, composition, structure, and morphological characteristics of the passive layer formed on the anode surface and the influence of the passive layer on the ferrate synthesis efficiency.
- Study on the factors affecting the stability and kinetics of the ferrate decomposition process.
- Study on the treatment of azo dyes with ferrate solution: study the factors affecting the removal efficiency (treatment time, molar ratio of ferrate/dye, temperature, inorganic ions).

CHAPTER 1. OVERVIEW

1.1. Background of ferrate

Ferrate(VI) is a compound of iron in which iron has an oxidation state of +6. The reduction potential of Fe(VI)/Fe(III) is up to 2.2 V in an acidic environment, so ferrate(VI) has a very strong oxidizing property and can decompose many toxic organic and inorganic substances in water sources. Therefore, ferrate(VI) has high potential in solving environmental problems. Ferrate is quite stable in the solid state, but in an aqueous environment, ferrate is unstable and easily decomposes into iron(III).

There are three methods in the synthesis of ferrate(VI) including: thermal method, wet method, and electrochemical method. In which the electrochemical method is used in many studies because it is a simple method, does not use chemicals and does not have toxic by-products, low cost... In addition, the electrochemical method can be used to synthesize ferrate in-situ to directly treat polluted wastewater sources.

1.2. Application of ferrate

Ferrate is a versatile oxidizing agent, playing many roles in wastewater treatment processes including oxidizing, disinfecting, and coagulating. Ferrate (FeO_4^{2-}) is a very strong oxidizing agent, so it is highly effective in treating toxic organic and inorganic substances in many water sources. The product of the ferrate reduction process is iron(III) hydroxide, an environmentally friendly coagulant capable of removing suspended solids and pollutants such as arsenic(V), cadmium(II), and copper(II). In addition, it is also an effective disinfectant, capable of eliminating pathogenic microorganisms such as viruses, bacteria, and fungi. Thanks to these outstanding advantages, ferrate has been extensively studied in the field of water and wastewater treatment.

1.3. Research background in worldwide and Vietnam

Currently, many research groups around the world have focused on synthesizing ferrate by electrochemical methods, developing on-site ferrate production systems, and applying them in water and wastewater treatment. Additionally, the application of ferrate in treating toxic, difficult-to-decompose organic substances, and chlorine-resistant viruses has also been researched and shown good treatment efficiency. In Vietnam, research on ferrate is still limited, and there has been little or no work on its electrochemical synthesis by domestic research groups.

CHAPTER 2. EXPERIMENT AND RESEACH METHODS

2.1. Experiment

Anode materials

The anode electrodes used for ferrate synthesis via the electrochemical method were fabricated from three materials: CT3 steel (mild steel – MS), grey cast iron (GCI), and ductile iron (DI). These materials were sourced from Hanoi Mechanical Limited Company, Vietnam. The composition of these materials is presented in Table 2.1

Table 2.1. Composition of anode materials using for ferrate electrochemical synthesis.

Materials	Mass composition (%)					
	Fe	C	Si	P	S	Mn
DI	93.701	3.650	2.330	0.010	0.009	0.300
GCI	92.480	5.214	1.778	0.011	0.021	0.496
MS	98.843	0.268	0.265	0.023	0.021	0.580

Ferrate synthesis

Note:

- (1)- Electrochemical workstation
- (2)- Magnetic stirrer
- (3)- Electrolyte
- (4)-Ag/AgCl reference electrode
- (5)- Anode
- (6)- Titanium counter electrode
- (7)- Membrane

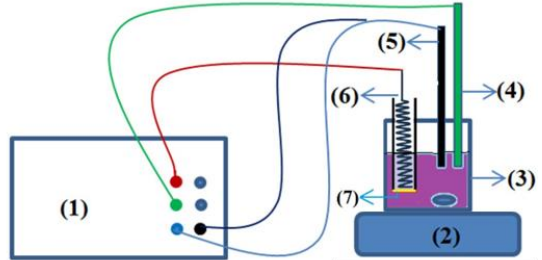


Figure 2.1. Schematic of the electrochemical cell of ferrate synthesis

Ferrate was synthesized by electrochemical method using a three-electrode system consisting of an Ag/AgCl reference electrode (saturated KCl), a titanium counter electrode, and working electrodes made from DI, GCI, and MS (Figure 2.1). The experiments were conducted using an IM6 electrochemical workstation (Zahner Elektrik, Germany), with variations in current density ranging from 10 to 50 mA/cm², NaOH electrolyte concentration from 8 to 16 M, and reaction temperature from 10 to 50 °C. The synthesized ferrate solution will be analyzed using UV-Vis spectroscopy

to determine its concentration. The electrochemical and physicochemical properties of the anode will be characterized both before and after the synthesis.

Treatment of azo dyes by ferrate

Reactive azo dyes, namely reactive red 195 (RR195) and methyl orange (MO), with an initial concentration of 50 mg/L, were treated using a ferrate(VI) solution at a concentration of 1500 ± 50 mg/L. The dye and ferrate solutions were mixed and stirred continuously at 500 rpm for the first 5 minutes, followed by static conditions for varying durations ranging from 0 to 55 minutes. The effects of pH (ranging from 1 to 9), temperature (10–50 °C), and the molar ratio of ferrate to dye were investigated.

2.2. Research methods

2.2.1. The electrochemical methods

The experiments for electrochemical ferrate synthesis and electrochemical characterization of the anode materials were conducted using an IM6 electrochemical workstation (Zahner Elektrik, Germany). The electrochemical measurements performed included:

- Cyclic Voltammetry (CV)
- Electrochemical Impedance Spectroscopy (EIS)
- Linear Sweep Voltammetry (LSV)

2.2.2. The physicochemical analysis methods

The changes in the surface structure of the anode before and after ferrate synthesis were evaluated using the following physicochemical analysis methods.

- Scanning electron microscopy (SEM) and energy dispersive X-ray spectroscopy (EDS) were performed using a FE SEM Hitachi S-4800 (Japan).
- X-ray diffraction (XRD) was performed on a D8-ADVANCE (Germany)
- Raman spectroscopy was carried out on a LabRAM HR Evolution (HORIBA Scientific, Japan)

2.2.3. Method for analyzing the concentration of ferrate and azo dyes

The concentrations of ferrate and dyes before and after treatment were determined by UV-Vis method on Perkin Elmer UV/Vis spectrometer Lambda 35 (USA) and Hach-DR6000 (USA).

CHAPTER 3. RESULTS AND DISCUSSION

3.1. Study on ferrate synthesis by electrochemical method

3.1.1. Anode material selection

Study on the electrochemical characteristics of anode materials

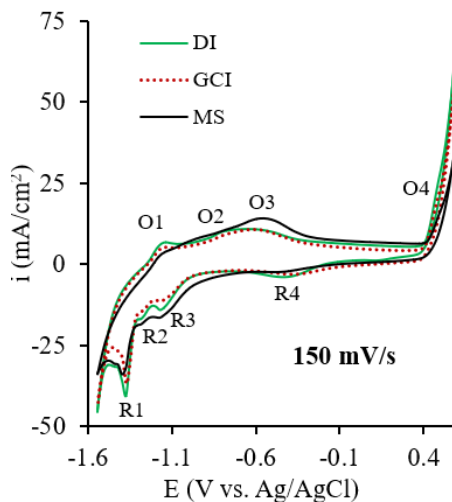


Figure 3.1. CV curves of DI, GCI, MS in 14 M NaOH solution.

Figure 3.1 shows the cyclic voltammetry (CV) curves of the anode electrodes in 14 M NaOH solution. The results indicate that there are four oxidation peaks and a shoulder (O1, O2, O3, and O4) on the anode branch and four reduction peaks (R1, R2, R3, and R4) on the cathode branch. In which the 4 oxidation peaks O1, O2, O3, O4 correspond to each process of changing the oxidation number of iron in the direction of increasing potential as follows: $\text{Fe} \rightarrow \text{Fe(II)} \rightarrow \text{Fe}_3\text{O}_4 \rightarrow \text{Fe(III)} \rightarrow \text{Fe(VI)}$.

Thus, the oxidation peaks O1, O2, and O3 correspond to the formation of intermediate species (Fe(II), Fe_3O_4 , Fe(III)), while the O4 peak is specifically associated with the formation of ferrate (Fe(VI)).

Comparing the CV spectra between three electrodes MS, GCI, DI at the same scanning speed of 150 mV/s shows that the MS anode has the highest peak pair (O3, R3) and the lowest peak pair (O4, R4) while the DI anode has the highest peak pair (O4, R4). This evidence shows that the formation of the passive layer on MS is easier and the formation of ferrate on MS is more difficult than the remaining electrodes. On the contrary, the ability to form ferrate on DI is the easiest.

The Bode plots of the anode materials at different temperatures are shown in Figures 3.2a–c. Based on these results, the Z impedance values at a frequency of 10 mHz were determined and presented in Figure 3.2d. The results indicate that Z values at 10 mHz decreased for all materials as the temperature increased from 10 °C to 50 °C. Specifically, Z value of DI decreased from 768 to 164 Ω , GCI from 932 to 173 Ω , and MS from 2350 to 159 Ω . These findings suggested that higher temperatures enhanced the oxidation of iron. Moreover, a comparison among the anode materials shows that DI consistently exhibited the lowest impedance across all temperatures, indicating that DI possesses favorable electrochemical properties for ferrate synthesis.

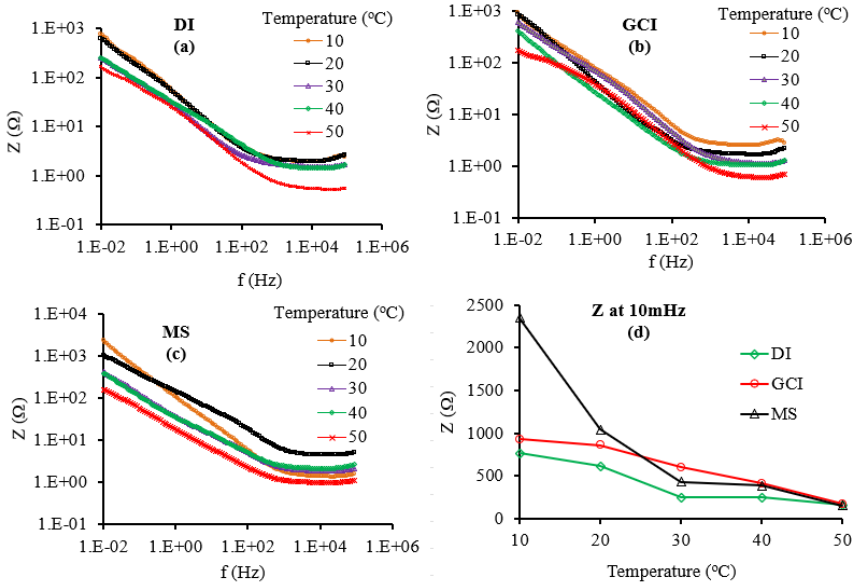


Figure 3.2. The Bode plots at different temperatures of (a) DI, (b) GCI, (c) MS and (d) Impedance values at 10 mHz.

Effect of anode material on the ferrate synthesis process

The results in Figure 3.3 demonstrated that ferrate concentration and synthesis yield increased markedly as the temperature rose from 10 °C to 40 °C, followed by a decline when the temperature was increased to 50 °C across all electrode types. Among the tested anodes, DI consistently

produced the highest ferrate concentration, while MS yielded the lowest at all temperatures. At 40 °C, the ferrate concentrations achieved were 437 mg/L (DI), 342 mg/L (GCI), and 328 mg/L (MS). The DI anode also exhibited the highest synthesis yield, reaching 74 % at 40 °C. These findings suggest that DI is a promising material for anode fabrication in electrochemical ferrate synthesis systems. The optimal temperature range for ferrate synthesis using nodular cast iron anodes is between 30 °C and 40 °C.

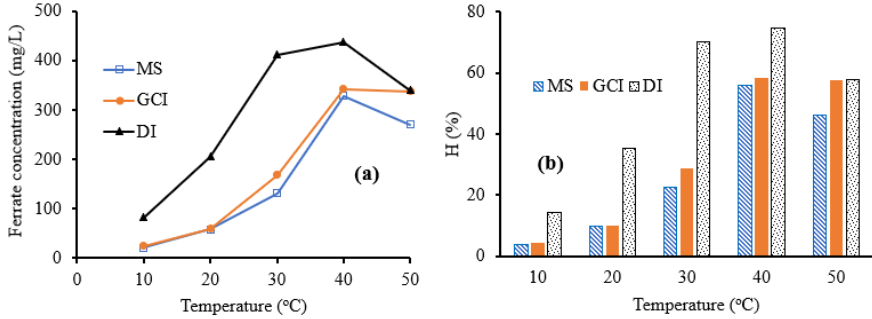


Figure 3.3. Effect of anode materials on (a) ferrate concentration, and (b) synthesis efficiency

Study on structural and morphological characteristic of anode materials

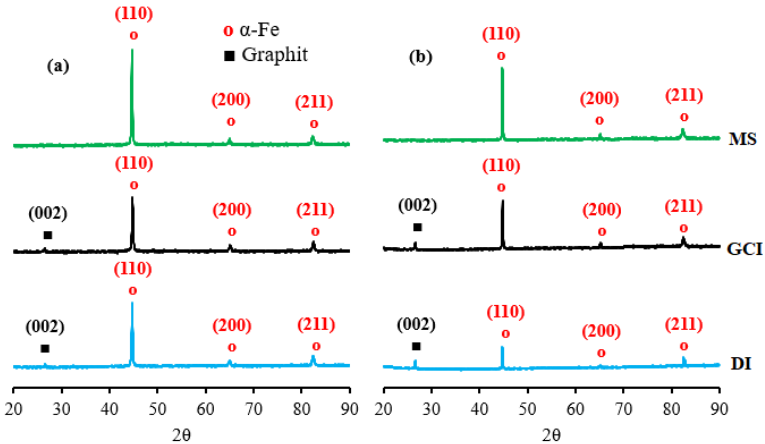


Figure 3.4. XRD patterns of DI, GCI and MS (a) before and (b) after 180 minutes ferrate electrochemical synthesis.

Figure 3.4 shows that after 180 minutes of electrolysis, the characteristic peaks corresponding to the ferrite structure on all materials significantly decreased. This reduction is attributed to the accumulation of iron oxide and hydroxide products on the anode surface.

SEM images after 180 minutes of electrolysis for DI and GCI electrodes (Figures 3.5d and 3.5e) reveal that severe corrosion occurs at the interface between the graphite and ferrite phases. This phenomenon is explained by these interfacial regions having less stable crystal structures, making them more susceptible to electrochemical corrosion. In addition, DI's spherical graphite structure is more porous, allowing deeper electrolyte infiltration, which expands the active interface and enhances mass transport. As a result, DI materials exhibit higher ferrate synthesis efficiency compared to MS and GCI.

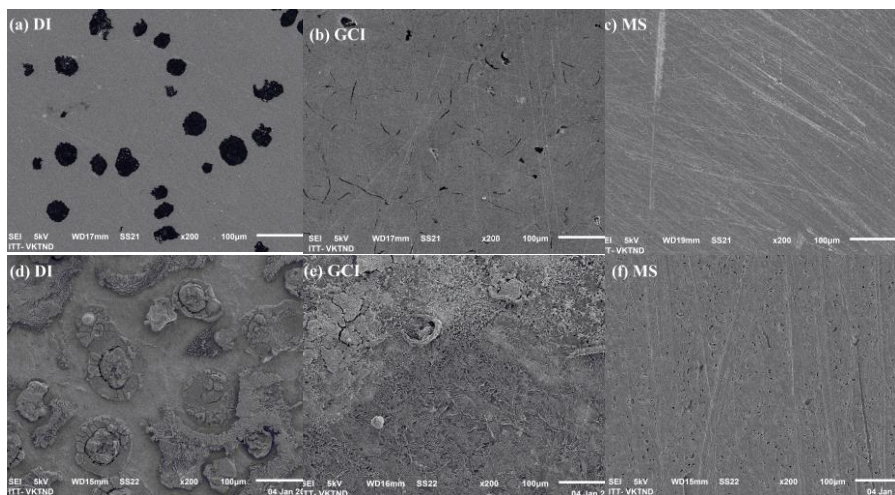


Figure 3.5. SEM images of anode materials (a,b,c) before, and (d,e,f) after 180 minutes ferrate electrochemical synthesis.

3.1.2. Study on the synthesis conditions of ferrate by electrochemical method using ductile iron anode.

Important variables affecting ferrate concentration and synthesis efficiency in electrochemical ferrate synthesis include electrode surface area-to-volume ratio (S/V), current density, electrolysis time, and electrolyte concentration. To optimize ferrate production using ductile iron anodes, each

of these variables was systematically investigated. The resulting performance data are presented in Figures 3.6 and 3.7.

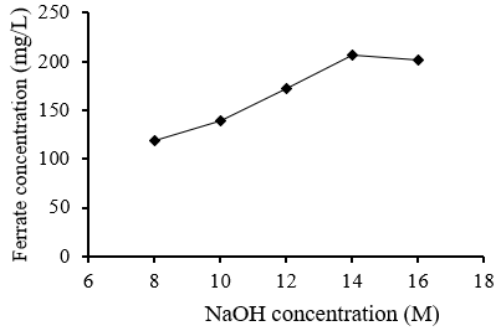


Figure 3.6. Effect of NaOH concentration on ferrate synthesis process.

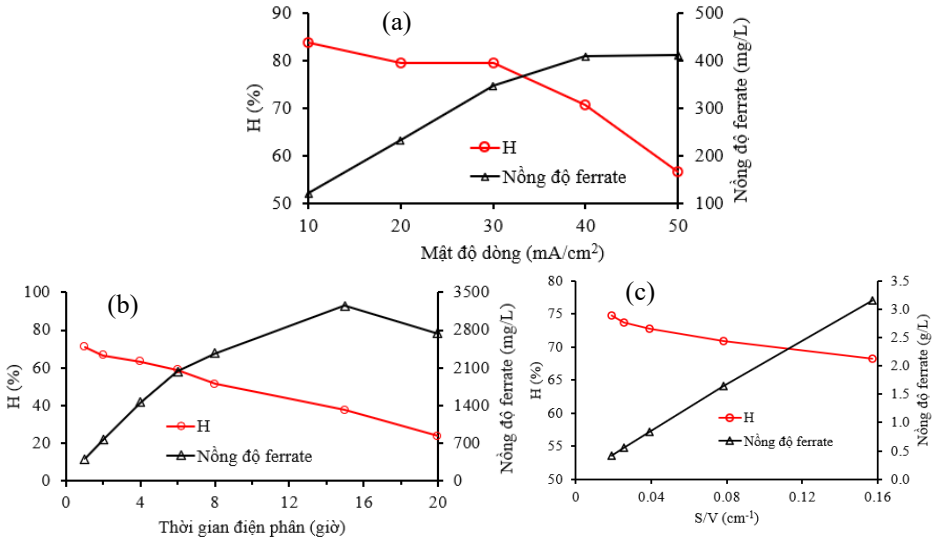


Figure 3.7. Effect of (a) current density, (b) electrolysis time, (c) S/V ratio on ferrate synthesis process.

Figure 3.6 shows that increasing the NaOH concentration from 8 to 14 M significantly enhances the ferrate concentration, reaching nearly 200 mg/L at 14 M. However, further increasing the NaOH concentration to 16 M results in a slight decrease in ferrate yield. Therefore, 14 M NaOH is

identified as the optimal electrolyte concentration for electrochemical ferrate synthesis using DI anode.

Figure 3.7a shows the effect of current density on the ferrate concentration and synthesis efficiency. Increasing the current density from 10 to 40 mA/cm² resulted in a ferrate concentration increase from 120.45 to 407.87 mg/L, accompanied by a decrease in synthesis efficiency from 83.75 to 70.65 %. Further increasing the current density to 50 mA/cm² caused a slight drop in ferrate concentration and a sharp fall in efficiency to 56.55 %. At high current density, the vigorous oxygen evolution reaction lead to bubble coverage on the anode surface, which restrict interface contact between the electrode and electrolyte. Consequently, 40 mA/cm² was determined as the optimal current density for ferrate synthesis in 14 M NaOH.

Figure 3.7b shows the dependence of ferrate concentration and synthesis efficiency on electrolysis time. In the initial phase (1–6 h), the ferrate concentration increased rapidly from 408 to 2035 mg/L, while the synthesis efficiency showed a slight decline from 74 to 60 %. In the second stage from 6 to 15 h, ferrate concentration increased more slowly and synthesis efficiency decreased more rapidly than in the previous stage. In the final stage from 15 to 20 h, both the synthesis efficiency and ferrate concentration declined. Therefore, to maintain a synthesis efficiency above 60 %, the electrolysis duration should be kept under 6 hours.

The S/V ratio is a critical factor influencing the electrochemical ferrate synthesis process. As shown in Figure 3.7c, increasing the S/V ratio from 0.019 to 0.157 cm⁻¹ raised the ferrate concentration over sevenfold, whereas the efficiency dropped by approximately 10 %. Despite this minor decrease in efficiency, a higher S/V ratio is advantageous, as it allows the desired ferrate concentration to be achieved in a shorter electrolysis time.

The above results indicate that the optimal conditions for ferrate synthesis using a ductile iron anode are a 14 M NaOH electrolyte solution, a current density of 40 mA/cm², and an electrolysis time of less than 6 hours, S/V ratio of 0,08 cm⁻¹.

3.2. Study on the formation passive layer on the ductile iron anode surface over time.

3.2.1. Study on the structural and morphological changes of the ductile iron anode over time.

Figure 3.8 shows the XRD patterns of DI anodes before and after electrolysis for 2, 6, and 15 hours. The characteristic diffraction peaks of the ferrite (α -Fe) crystal structure appeared in both samples before and after electrolysis for 2 and 6 hours. However, the intensity of these peaks gradually decreased with increasing electrolysis time and disappeared in the DI sample after 15 hours of electrolysis. This reduction is attributed to the formation of an amorphous iron oxide passivation layer that thickens over time. This phenomenon is demonstrated in the SEM image (Figure 3.9), where a passivation layer completely covers the anode surface after 15 hours of electrolysis.

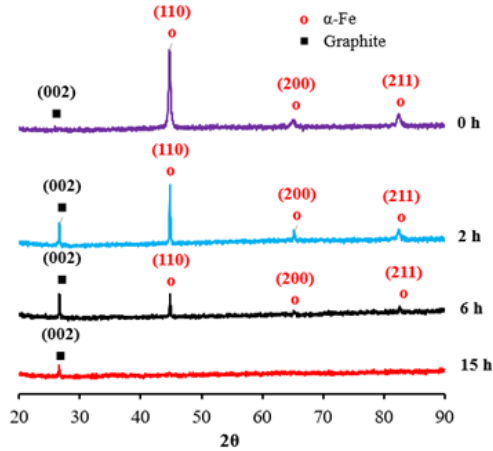


Figure 3.8. XRD patterns of the DI anodes before and after different electrolysis times.

Figure 3.9 presents the SEM images of the DI anodes before and after electrolysis. Oxidation occurs strongly around the spherical graphite particles, forming a fine-textured passive layer (region B) surrounding the nodules (region A); additionally, the porous passive layer was also formed in the outer area of the graphite nodules (region C). Increasing electrolysis time from 2 to 15 h, the area of region B expanded, whereas regions A and C narrowed.

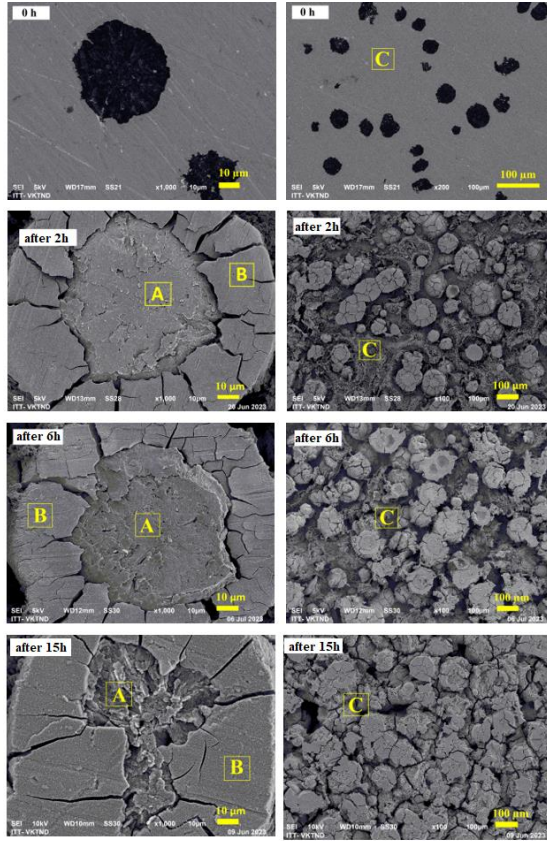


Figure 3.9. SEM images of the DI anodes before and after different electrolysis times.

3.2.2. Study on composition of passive layer

The elemental composition determined by EDS method on the DI anode surface in regions A, B, C at different electrolysis times is summarized in Table 3.2.

After electrolysis time of 2 and 6 hours, region A was mainly composed of carbon (95.2 % and 94.1 %). After 15 hours of electrolysis, carbon composition dropped to 19.7 %, while composition of Fe and O increased, indicating iron oxide formation on the graphite nodules surface.

In region B, the carbon content remains nearly constant at around 10 % across different electrolysis durations. The mass ratio between iron and

oxygen varies slightly from 1.9 to 2.1, predicting that the passive layer in region B likely consists of a mixture of FeOOH , Fe_2O_3 , and Fe_3O_4 .

In region C, the iron component was still dominant after 2 h of electrolysis (80.8 %), and oxygen accounted for 11.2 %, so only a small amount of iron oxide was formed on the surface. The iron component decreased and the oxygen component gradually increased with increasing electrolysis time to 6 and 15 h, indicating that the iron oxide layer on region C thickened over time.

Table 3.1. Mass composition of elements on the DI anodes surface after different electrolysis times.

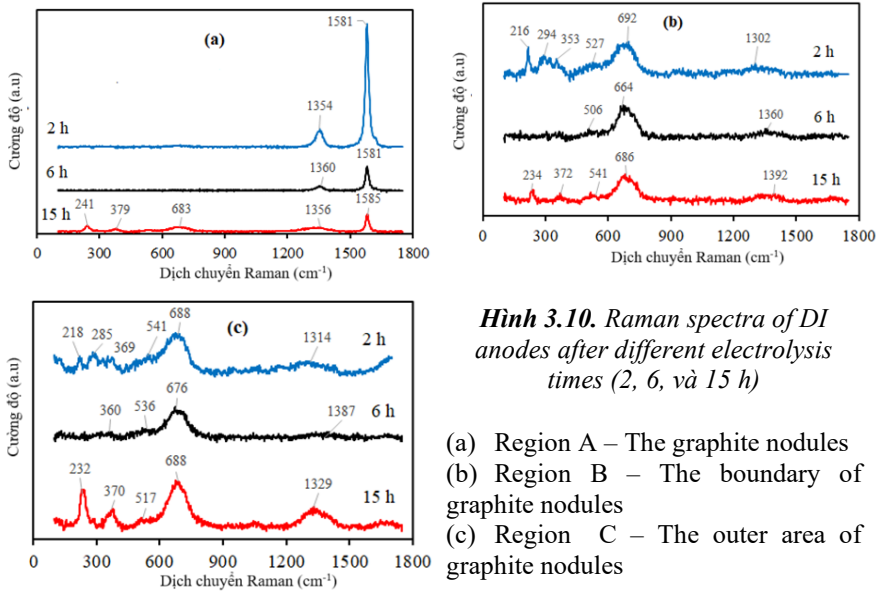
Area	Electrolysis time (h)	Mass composition (wt %)				
		Fe	O	C	Si	Na
A	2	1.7	3.1	95.2	-	-
	6	2.1	3.6	94.1	0.2	-
	15	52.3	25.5	19.7	0.2	1.9
B	2	57.5	26.9	10.5	3.0	2.2
	6	54.4	28.6	10.7	3.0	2.3
	15	57.8	27.9	9.6	0.7	3.2
C	2	80.8	11.3	6.1	1.1	0.7
	6	68.1	15.5	12.6	2.0	0.8
	15	59.1	28.6	8.3	0.4	2.8

The Raman spectra given in Figure 3.10 show the formation of iron oxides on the surface of DI after 2, 6 and 15 h of electrolysis.

The Raman spectra of Region A show graphite peaks at ~ 1580 and $\sim 1355 \text{ cm}^{-1}$ after 2 and 6 hours of electrolysis. After 15 hours, in addition to the graphite peaks at 1585 and 1356 cm^{-1} , new peaks appear at 241 and 379 cm^{-1} ($\alpha\text{-Fe}_2\text{O}_3$) and at 683 cm^{-1} (Fe_3O_4). This suggests that prolonged electrolysis leads to graphite nodules being covered by iron oxides from ferrate decomposition.

The Raman spectra in Figure 3.10c, similar to Figure 3.10b, show that after 2 hours of electrolysis, the regions B, C contained a mixture of $\alpha\text{-FeOOH}$, $\alpha\text{-Fe}_2\text{O}_3$, and Fe_3O_4 . However, after 6 and 15 hours, only $\alpha\text{-Fe}_2\text{O}_3$ and Fe_3O_4 are detected. Notably, the Fe_3O_4 peaks are consistently more

intense than those of $\alpha\text{-Fe}_2\text{O}_3$ and FeOOH at all electrolysis durations. This suggests that Fe_3O_4 is the predominant component of the passive layer, which is consistent CV curves analysis (Figure 3.11).



Hình 3.10. Raman spectra of DI anodes after different electrolysis times (2, 6, và 15 h)

3.2.3. Ảnh hưởng của lớp thụ động tới tính chất điện hóa của anot

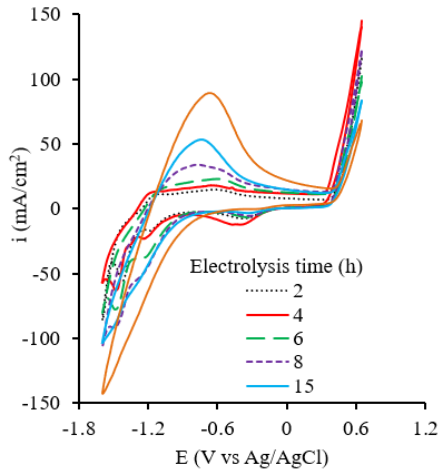


Figure 3.11. CV curves of DI anode after different electrolysis times.

CV and EIS spectra were measured at different electrolysis times to evaluate the impact of the passivation layer on the electrochemical properties of the anode. The results are shown in Figures 3.11 and 3.12.

After electrolysis time greater than 6 hours, the CV curves mainly show the O₂ peak, O₄ peak shoulder and R₄ peak. Increasing electrolysis time from 8 to 20 hours raised the height of the O₂ peak, but decreased the height of O₄ peak shoulder and R₄ peak. Therefore, with electrolysis time greater than 6 hours, the passivation layer on the DI anode will significantly inhibit the formation of ferrate.

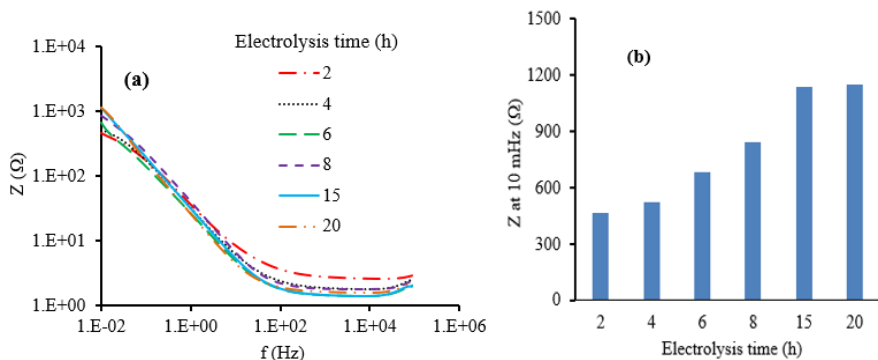


Figure 3.12. Bode plots of DI anode at different electrolysis times.

The impedance values at low frequency of 10 mHz increased with rising electrolysis time from 2 to 20 hours because of the developing of the passive layer on the anode surface. This result is consistent with the CV measurement results presented above.

3.2.4. Effect of passive layer on ferrate synthesis process

As shown in Figure 3.13, the ferrate concentration remained relatively stable in the range of 410 to 426 mg/L during the first 1–6 hours of electrolysis. However, it dropped significantly after 8–20 hours, with a 46 % decrease at 20 hours. The optimal operating time of the electrolysis cycle for the DI anode was 6 hours. Therefore, after about 6 hours of operation, the anode needs to be cleaned on the surface to remove the passive layer to ensure that the ferrate synthesis process takes place effectively.

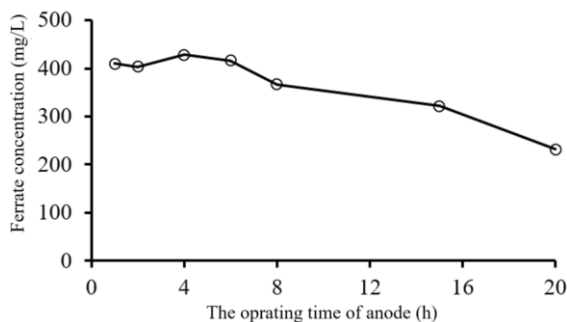


Figure 3.13. Effect of operating time of anode on ferrate concentration.

3.3. Study on the stability of synthesized ferrate solutions

3.3.1. Factors affecting the stability

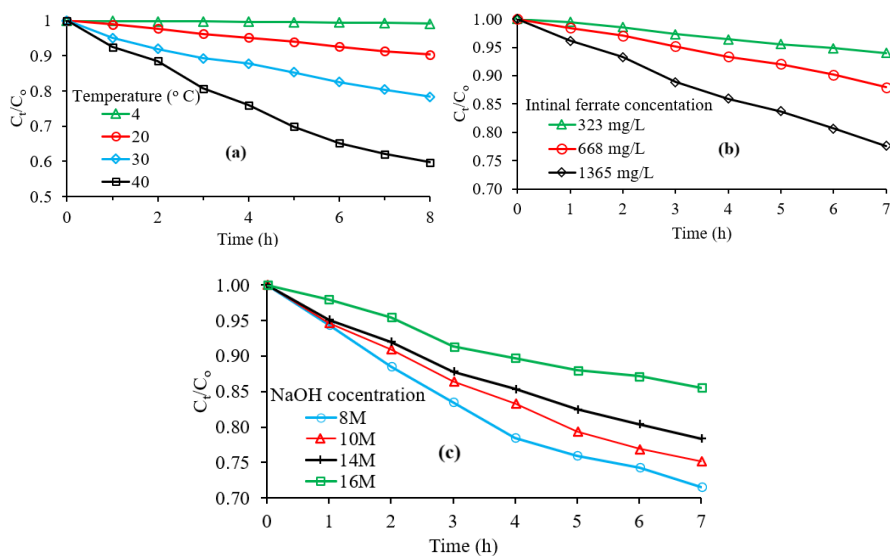


Figure 3.14. Effect of (a) temperature, (b) initial ferrate concentration, and (c) NaOH concentration on the stability of ferrate solution.

Figure 3.14a illustrates the impact of temperature on ferrate solution stability. The results indicate that ferrate decomposed more rapidly at higher temperatures. At 4 °C, decomposition was minimal, with ferrate concentration remaining nearly constant after 8 hours. In contrast, significantly greater decomposition occurred at 20 °C, 30 °C, and 40 °C.

Therefore, to minimize self-decomposition, unused ferrate should be stored at low temperatures.

Figure 3.14b shows that the decomposition rate of ferrate depends on its initial concentration, the higher the initial concentration, the faster the decomposition rate. Specifically, after 7 hours, the ferrate of the sample with an initial concentration of 323 mg/L decomposed by about 6 %, while for the sample with an initial concentration of 1365 mg/L, this value increased to nearly 23 %.

Figure 3.14c illustrates the effect of NaOH concentration on ferrate stability. The decomposition rate of ferrate increases as NaOH concentration decreases. After 7 hours, approximately 30 % of ferrate decomposed in 8 M NaOH solution—about twice the amount compared to that in 16 M NaOH.

3.3.2. Kinetics of ferrate solution decomposition

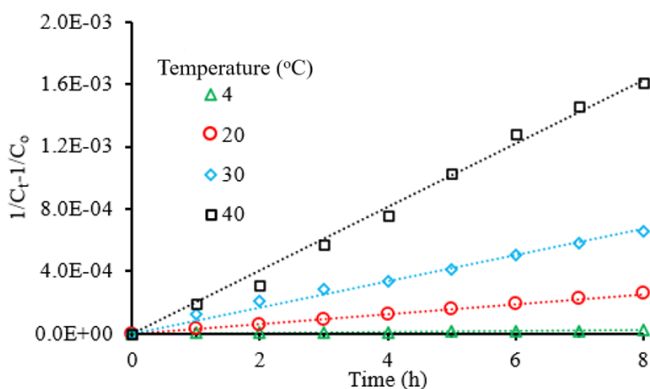


Figure 3.15. Relationship between $\frac{1}{C_t} - \frac{1}{C_0}$ and time.

The relationship between $\frac{1}{C_t} - \frac{1}{C_0}$ and t at different temperatures is shown in Figure 3.15. The linear trend observed, with a coefficient of determination R^2 greater than 0.99 at all temperatures, confirms that the ferrate decomposition in 14 M NaOH follows a second-order kinetic model. The slope of each line corresponds to the reaction rate constant, as summarized in Table 3.2. As temperature increases, the rate constant rises markedly about 16-fold from 4 to 20 °C and nearly 100-fold from 4 to 40 °C, demonstrating the strong temperature dependence of the decomposition rate.

Table 3.2. Rate constants of ferrate decomposition reaction at different temperatures.

T	k ₂		R ²
°C	(mg/L) ⁻¹ h ⁻¹	M ⁻¹ .s ⁻¹	
4	2.03x10 ⁻⁶	4.70x10 ⁻⁹	0.9945
20	3.16x10 ⁻⁵	7.31x10 ⁻⁸	0.9989
30	8.42x10 ⁻⁵	1.95x10 ⁻⁷	0.9969
40	2.03x10 ⁻⁴	4.70x10 ⁻⁷	0.9977

3.4. Study on treatment of azo dyes methyl orange (MO) and reactive red 195 (RR195)

3.4.1. Study on optimal conditions for dye treatment

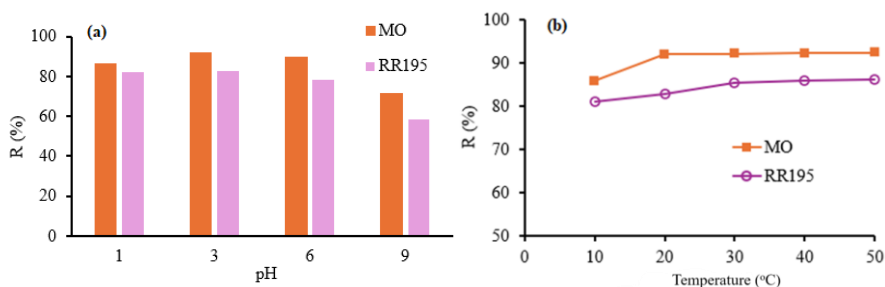


Figure 3.16. Effect of (a) pH, and (b) temperature on MO and RR195 removal efficiency.

pH is a critical factor in the treatment of azo dyes with ferrate, as it influences both the oxidizing power and the decomposition rate of ferrate. As illustrated in Figure 3.16, the dye removal efficiency is higher under acidic conditions than in alkaline conditions, with optimal performance observed at pH 3. In contrast, temperature has a minimal effect on the dye treatment efficiency, as shown in Figure 3.16b.

Figure 3.17 shows the effect of ferrate/dyes molar ratios on treatment efficiency over time. The oxidation reaction of MO and RR 195 of ferrate occurs mainly in the first 3-5 minutes. The RR 195 removal efficiency

reaches 96 % after 3 minutes at the molar ratio of $\text{Fe(VI)}/\text{RR 195} = 24/1.0$, the MO removal efficiency reaches 99.3 % after 3 minutes at the molar ratio of $\text{Fe(VI)}:\text{MO}$ of 8.5/1.0.

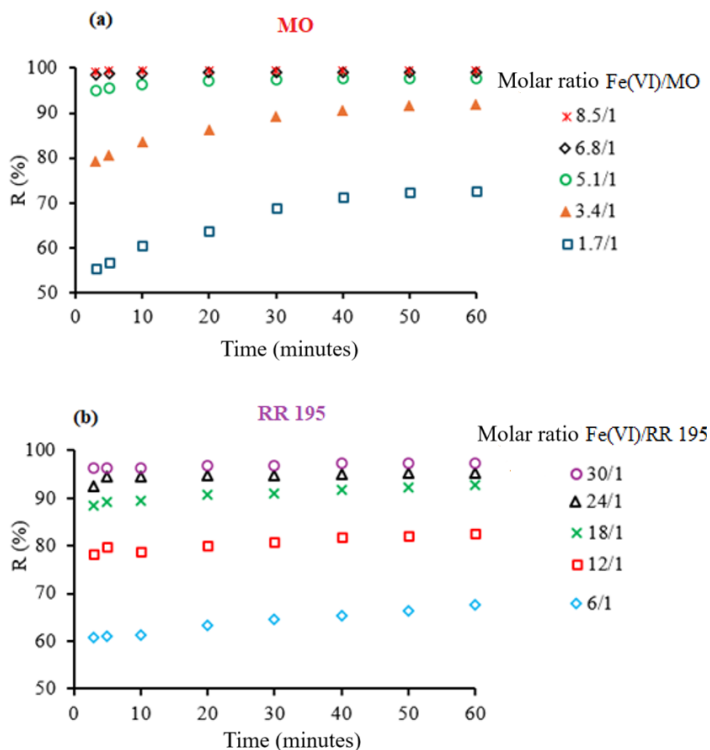


Figure 3.17. Effect of molar ratio of ferrate/dye on degradation efficiency
a) MO, b) RR195.

3.4.2. Effect of some inorganic ions on the dye treatment process

In addition to organic dyes, dye wastewater also contains various inorganic ions such as Cu^{2+} , Mg^{2+} , Fe^{3+} , Mn^{2+} , Cl^- , NO_3^- , CO_3^{2-} , and SO_4^{2-} . Figures 3.18 and 3.19 illustrate the influence of some anions and cations on the dye removal efficiency.

The results indicate that Fe^{3+} and Mg^{2+} ions almost did not affect the dye degradation efficiency, whereas the presence of Cu^{2+} ions led to a decrease in treatment performance. In contrast, some anions such as Cl^- and NO_3^- enhanced the dye removal efficiency

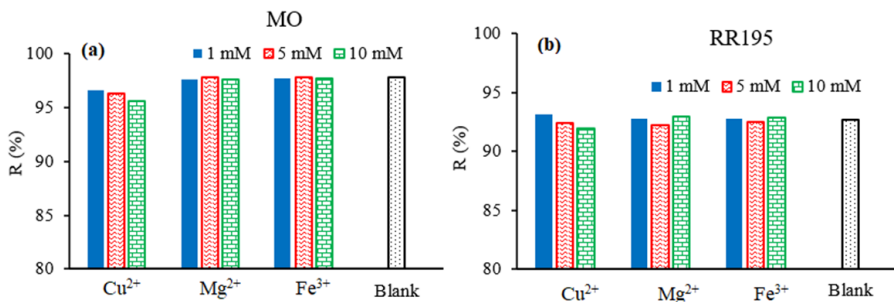


Figure 3.18. Effect of cations on the degradation efficiency of (a) MO, (b) RR195 by ferrate.

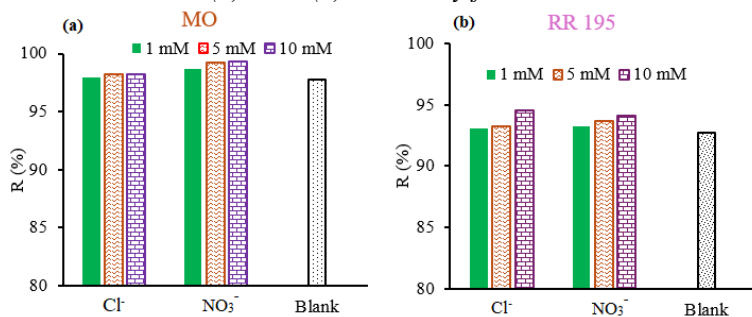


Figure 3.19. Effect of anions on the degradation efficiency of (a) MO, (b) RR195 by ferrate.

3.4.3. Comparison of the efficiency of azo dye decomposition by ferrate with other methods

To remove MO and RR195 from wastewater, many treatment methods have been used, such as adsorption, chemical coagulation, photocatalysis, electrocatalysis, and biological methods. However, adsorption and chemical coagulation transfer dyes from the liquid phase to the solid phase, thereby causing secondary pollution. Biological methods are not suitable for MO treatment due to their low biodegradability. Tables 3.3 and 3.4 compare different methods for MO and RR195 treatment. The results show that ferrate (VI) has better treatment performance in a short time. Moreover, because ferrate is a green oxidant, easy to synthesize, and low cost, ferrate (VI) becomes a viable option for the removal of azo dyes in textile wastewater.

Bảng 3.3. Comparison of MO treatment methods.

Method/Material	Treatment time (minutes)	Removal efficiency (%)
Oxidation ($O_3/K_2S_2O_8$)	50	98.6
Fenton reaction (H_2O_2/Fe^{2+} - UV)	15	97.8
Photocatalysis [$FemIL@SiO_2@Mag$] $_2MoO_4$	30	99.0
Photocatalysis (Fe_3O_4/TiO_2)	60	90.3
Photocatalysis (MoS_2/Fe_3O_4)	100	79.5
Electrocatalytic oxidation ($PbO_2 - TiO_2$)	50	99.3
Electrocatalytic oxidation ($Ti/SnO_2 - Sb_2O_3 / PbO_2 - TiO_2$)	240	95.5
Adsorption (MOF: Ni-doped ZIF-67)	120	82.9
Photoelectrocatalytic process (Reduced – TiO_2)	30	98.4
Advance oxidation (ferrate(VI))	3	99.3
	60	99.4

Bảng 3.4. Comparison of RR195 treatment methods.

Method/Material	Treatment time (minutes)	Removal efficiency (%)
Electrochemical oxidation (graphite electrode)	60	93.9
Electro-Fenton reaction (Fe_3O_4/rGO)	60	93.3
Catalytic ozonation (nZVI-Ca-Alginate Beads)	90	99.0
Electro ozone generation ($Ti/TiHx/SnO_2-Sb_2O_5-NiO-CNT$ electrode)	30	96.0
Photocatalysis ($Ag/TiO_2/Fe_3O_4$ nanocomposite)	30	98.0
Adsorption (chitosan-cellulose)	320	97.2
Adsorption (crosslinked oxalic acid/chitosan hydrogels)	600	90.6
Advance oxidation (ferrate(VI))	3	96.3
	60	97.3

CONCLUSIONS

1. Ferrate solution was successfully synthesized using galvanostatic technique. Compared to gray cast iron and CT3 steel, the ductile iron material had a substantially greater ferrate synthesis efficiency, reaching 74 % at 40 °C. The optimal parameters for ferrate production using ductile iron anode were: 14 M NaOH electrolyte solution, current density 40 mA/cm², temperature 30-40 °C, and S/V ratio 0.08 cm⁻¹.
2. SEM images and XRD patterns confirmed the formation and progressive thickening of a passive layer on the surface of ductile iron anodes during electrochemical ferrate synthesis. CV, Raman, and EDS spectra showed that the composition of the passive layer included a mixture of iron oxides FeOOH, Fe₂O₃, and Fe₃O₄, of which Fe₃O₄ accounted for the majority. EIS and CV results further indicated that the passive layer impeded electrochemical activity on the anode surface, leading to reduced ferrate synthesis efficiency. The optimal electrolysis duration for ductile iron anodes was determined to be 6 hours, after which surface treatment is required to remove the passive layer and maintain performance.
3. The stability of ferrate solution depends on factors including: temperature, NaOH concentration and initial ferrate concentration. As the temperature and initial ferrate concentration increase, the stability decreases, conversely, as the NaOH concentration increases, the stability increases. Ferrate solution is optimally stored at 4 °C and NaOH concentration of 14-16 M.
4. The treatment of MO and RR195 by ferrate depends on both pH and the ferrate/dye molar ratio. At the optimal pH of 3, removal efficiency exceeds 90 % when the Fe(VI)/MO ratio is above 5.1/1.0 and Fe(VI)/RR195 is above 18/1.0. The degradation reactions of MO and RR195 by ferrate(VI) occur mainly in the initial minutes. The removal efficiency of RR195 reaches 93 % after 3 minutes at a Fe(VI)/RR195 molar ratio of 24.1/1.0, while MO achieves 99.3 % removal after 3 minutes at a Fe(VI)/MO ratio of 8.5/1.0.

NEW CONTRIBUTIONS OF THE THESIS

1. Ferrate solution was successfully synthesized by an electrochemical method using low cost ductile iron as a novel anode material. The ductile iron anode exhibited high synthesis efficiency, reaching 74 % at 40 °C. Optimal electrochemical synthesis conditions were identified for ferrate generation using this anode material.
2. The study clarified the formation mechanism of the passive layer on the surface of ductile iron during electrochemical ferrate synthesis. Results revealed that Fe_3O_4 is the main component of this layer. Moreover, the passive layer was shown to reduce the efficiency of ferrate production.
3. The successful treatment of the azo dye Reactive Red 195 using ferrate was achieved at a molar ratio of ferrate/RR195 greater than 18/1. It was demonstrated that the dye degradation occurred rapidly, within just 3 to 5 minutes.